Lithuanian Journal of Physics, Vol. **53**, No. 2, pp. 118–125 (2013)

PHOTOLUMINESCENCE LIFETIMES IN GaAs/Al$_{0.3}$Ga$_{0.7}$As STRUCTURES DESIGNED FOR MICROWAVE AND TERAHERTZ DETECTORS

A. Čerškus [a, b], J. Kundrotas [a], V. Nargelienė [a], A. Sužiedėlis [a], S. Ašmontas [a],

J. Gradauskas [a], E. Johannessen [c], and A. Johannessen [c]

[a] *Semiconductor Physics Institute of Center for Physical Sciences and Technology, A. Goštauto 11, LT-01108 Vilnius, Lithuania*
[b] *Lithuanian University of Educational Sciences, Studentų 39, LT-08106 Vilnius, Lithuania*
[c] *Vestfold University College, Raveien 197, 3184 Borre, Norway*
E-mail: a_cerskus@yahoo.com

Received 2 July 2012; revised 15 October 2012; accepted 20 June 2013

This paper presents the photoluminescence spectra and light emission lifetimes in GaAs/Al$_{0.3}$Ga$_{0.7}$As structures designed for microwave and terahertz detectors. The photoluminescence and light emission lifetimes were investigated both before and after etching of the cap-layers, and possible mechanisms of carrier recombination are discussed. The characteristic time of the free exciton emission corresponds to 0.5 ns at a temperature of 3.6 K. The recombination lifetime of the free electron acceptor was measured to be 22–25 ns in GaAs structures and 4–15 ns in AlGaAs structures. The emission lifetime of deep Si level having 170 meV activation energy in AlGaAs layer was found to be equal to 40 ns. The excitonic photoluminescence maxima of n^+/n-GaAs and n^+/n-Al$_{0.3}$Ga$_{0.7}$As homojunction structures in comparison to n-GaAs and n-Al$_{0.3}$Ga$_{0.7}$As were shifted by approximately 200 ps. This suggested that the drift of free carriers is important in the formation of free excitons in n-GaAs and n-Al$_{0.3}$Ga$_{0.7}$As layers.

Keywords: GaAs, AlGaAs, homojunction, photoluminescence, lifetime, exciton, photoluminescence enhancement

PACS: 78.55.-m, 71.55.Eq, 71.35.-y

1. Introduction

The focus on radiation technology has in the recent years shifted from frequencies in the infrared region to the terahertz region. This spectral range has an enormous potential for applications such as biology, medicine, security, and wireless communications [1, 2]. However, the main challenge of utilizing the frequencies in this field is the lack of suitable and reliable terahertz sources and detectors. Hence, the current research in the field of communication technology aims to increase the operational bandwidth of its emitters and detectors. Though the greatest achievements have been reported in the visible, near-infrared, and microwave (MW) bands, the performance of existing device technology in the high-frequency MW region as well as in the terahertz (THz) range is still considered being modest. Therefore, a new generation of emitters [3, 4] and detectors [5, 6] based on n^+/n, n^+/i and p^+/i homojunctions or GaAs/AlGaAs heterostructures [7] has been proposed for operation in the MW and THz ranges. However, the characterization of these devices has not been fully investigated so far.

We have developed a novel device model based on GaAs and AlGaAs structures for the detection of radiation in the broad band region from MW to THz [8]. This paper presents a continuous wave photoluminescence (PL) and time-resolved photoluminescence characterization of these structures.

The possible mechanisms of carrier recombination are discussed and an emphasis is placed on the enhancement of the photoluminescence and the reduction of the excitonic emission lifetime observed in these structures.

2. Samples and experimental protocol

The structures were grown by molecular beam epitaxy (MBE) [9, 10] on a semi-insulating GaAs substrate. The active region consisted of two homojunctions: Si-doped n^+/n (or n/n^+) $Al_xGa_{1-x}As$ and n^+/n (or n/n^+) GaAs. The layered composition of the $GaAs/Al_xGa_{1-x}As$ structure is shown in Table 1. The samples #1 and #6 were grown with aluminum mole fraction $x = 0.3$ in the active region based on two different designs.

The time-integrated PL was measured by a fully automated monochromator FHR-1000 with the focal length of 1000 mm. The spectra were dispersed with blazed 1200 gr/mm grating, and the spectral dispersion was 0.8 nm/mm. The wavelength spectral resolution was 0.01 nm at a 10 μm exit slit width, or a correspondent energy spectral resolution was 0.02 meV at 820 nm and 0.03 meV at 645 nm. An Ar-ion laser was used as an excitation source. The excitation energy was in the region of 2.2–2.7 eV and the PL was detected by a thermoelectrically cooled GaAs photomultiplier operating in the photon counting regime.

The time-resolved PL measurements were carried out using a frequency-doubled diode-pumped Nd:LSB microchip solid-state laser with a 400 ps FWHM pulse width. The pulse repetition rate was 10 kHz with an average output power of 40 mW. The excitation wavelength was 531 nm (photon energy 2.3 eV). The PL was detected with a thermoelectrically cooled high efficiency extended-red multi-alkali cathode photomultiplier with an internal GHz preamplifier. The transient photoluminescence were measured using a time correlated single photon counting (TCSPC) system [11]. In order to avoid jitter, the measured signal was synchronized with a part of splitted exciting laser pulse.

The excitation intensity was changed by using neutral glass filters. The 1 W @4.2 K model SHI-4 closed cycle helium optical cryostat enabled to control the sample temperatures from ambient room temperature (300 K) down to 3.6 K. The cryostat was equipped with two thermometers: the first one was used to control operation of the equipment and the second measured temperature of the sample.

Chemical etching of the top layers was performed using a $H_3PO_4:H_2O_2:H_2O = 1:1:50$ solution. The degree of etching was controlled with a profilometer by leaving part of the sample unetched.

3. Experimental results

The PL spectra of $GaAs/Al_{0.3}Ga_{0.7}As$ structures at a temperature of 3.6 K using a laser excitation intensity of $I = 1.36$ W/cm^2 are presented in Fig. 1. One can resolve two parts of the spectra indicated by segments. The first one, below 1.57 eV, is attributed to GaAs layers. The emission below the forbidden energy gap, E_g(GaAs) = 1.519 eV, is related to the lightly doped GaAs layer. Lower energy transition at 1.49 eV, labelled *e-A*, is a recombination of a free electron with the residual acceptor. The transition at 1.515 eV is a well-known free exciton line [12] (marked as *X* in Fig. 1). The broad band from 1.5 to 1.57 eV is attributed to emission from the heavily doped GaAs layer (n^+-GaAs). This broad band nearly disappeared from the spectra when the

Table 1. The structure of the $GaAs/Al_{0.3}Ga_{0.7}As$ samples. N_D is donor concentration, h – layer thickness, N – quantum wells number.

#1	#6
n^+-GaAs, $N_D = 3 \times 10^{18}$ cm^{-3}, $h = 100$ nm	n^+-GaAs, $N_D = 2 \times 10^{18}$ cm^{-3}, $h = 250$ nm
n^+-$Al_{0.3}Ga_{0.7}As$, $N_D = 3 \times 10^{18}$ cm^{-3}, $h = 100$ nm	
n-$Al_{0.3}Ga_{0.7}As$, $N_D = 10^{16}$ cm^{-3}, $h = 300$ nm	n-GaAs, $N_D = 10^{16}$ cm^{-3}, $h = 300$ nm
n-GaAs, $N_D = 10^{16}$ cm^{-3}, $h = 300$ nm	n-$Al_{0.3}Ga_{0.7}As$, $N_D = 10^{16}$ cm^{-3}, $h = 300$ nm
n^+-GaAs, $N_D = 3 \times 10^{18}$ cm^{-3}, $h = 300$ nm	n^+-$Al_{0.3}Ga_{0.7}As$, $N_D = 6 \times 10^{18}$ cm^{-3}, $h = 300$ nm
i-$Al_{0.25}Ga_{0.75}As$, $h = 10$ nm, $N = 20$	i-$Al_{0.25}Ga_{0.75}As$, $h = 10$ nm, $N = 20$
i-GaAs, $h = 10$ nm, $N = 20$	i-GaAs, $h = 10$ nm, $N = 20$
i-GaAs, $h = 200$ nm	i-GaAs, $h = 200$ nm
SI GaAs substrate	SI GaAs substrate

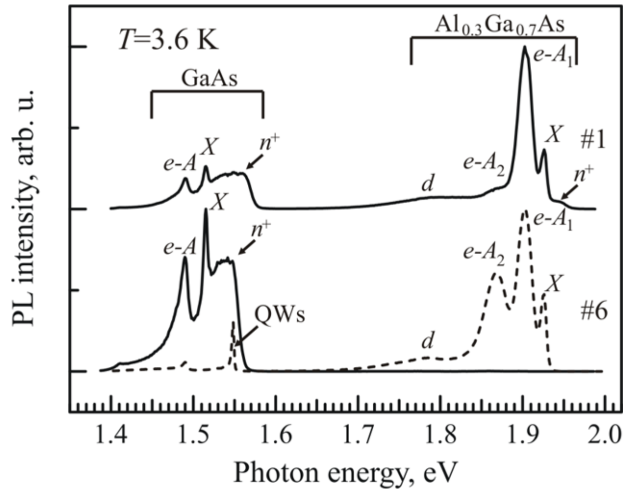

Fig. 1. The PL spectra of GaAs/$Al_{0.3}Ga_{0.7}As$ structures at a temperature of 3.6 K and laser intensity of I = 1.36 W/cm^2 for two samples (#1 and #6) of different design. The symbol X indicates excitonic emission, e-A, e-A_1, e-A_2 are radiative emissions related to acceptor impurities, and d is emission related with defects in the $Al_{0.3}Ga_{0.7}As$ region. The symbol n^+ denotes emission from the heavily doped GaAs or $Al_{0.3}Ga_{0.7}As$ layer. The dashed line shows the photoluminescence spectrum for sample #6 after etching of n^+ and n GaAs cap-layers. The symbol QWs denotes emission from multiple quantum wells formed in the buffer layer. The spectra are shifted along the vertical axis for clarity.

top n^+-GaAs layer was etched off. The radiation from multiple quantum wells (QWs) in the buffer layer at 1.547 eV is not clearly distinguished in Fig. 1. Clear excitonic lines of radiation from QWs were only observed after the partial or full etching of the top layers had been performed.

The second part of the PL spectra is associated with the $Al_{0.3}Ga_{0.7}As$ layers. This part of the spectrum can be interpreted as a superposition of two separate spectra arising from both the n^+-type and n-type $Al_xGa_{1-x}As$ layers. As Fig. 1 shows, this part of the spectrum consists of five broad peaks.

In order to measure the PL spectra lines from the $Al_{0.3}Ga_{0.7}As$ layers in sample #6, the n^+ and n GaAs cap-layers had to be removed. The spectrum is shown as a dotted line in Fig. 1. The high-energy broad peak n^+ is related to the radiation from n^+-$Al_xGa_{1-x}As$. We have measured the PL intensity of the X peak to be around 1.926 eV at 3.6 K. This PL intensity increases with temperature and has been identified as the excitonic line. Two other peaks, labelled as e-A_1 and e-A_2, found around 1.903 and 1.870 eV at a temperature of 3.6 K, have been found to saturate and disappear above 40 and 60 K, respectively. Consequently, they should be related to two different shallow impurities. The nature of the lowest energy broad peak d dominating at the liquid nitrogen temperature (77 K) can be also related to defects.

In a previous paper [13], the enhancement of PL emission intensity in n^+/n-GaAs and n^+/n-$Al_{0.3}Ga_{0.7}As$ homojunctions of one of these structures (sample #1) has been reported. Below we present PL decay transients in n^+/n-GaAs, n-GaAs, n^+/n-$Al_{0.3}Ga_{0.7}As$, and n-$Al_{0.3}Ga_{0.7}As$ parts of that structure. Figure 2 shows the PL time evolution of different emission bands in layers of (a) n^+/n-GaAs and (b) n-GaAs in sample #6 after conducting a pulsed laser excitation at a temperature of T = 3.6 K. The curves were fitted by incorporating one or two exponential decay constants, and the characteristic decay times were extracted. Short lifetimes were extracted after application of deconvolution algorithm for signal processing [14, 15]. As a result, the free excitonic emission decay time of the n-GaAs layer is equal to τ_X(n-GaAs) = 0.4 ns and that of the n^+/n-GaAs structure is slightly longer and equal to τ_X(n^+/n-GaAs) = 0.6 ns at 3.6 K. The free electron-acceptor decay consists of two parts.

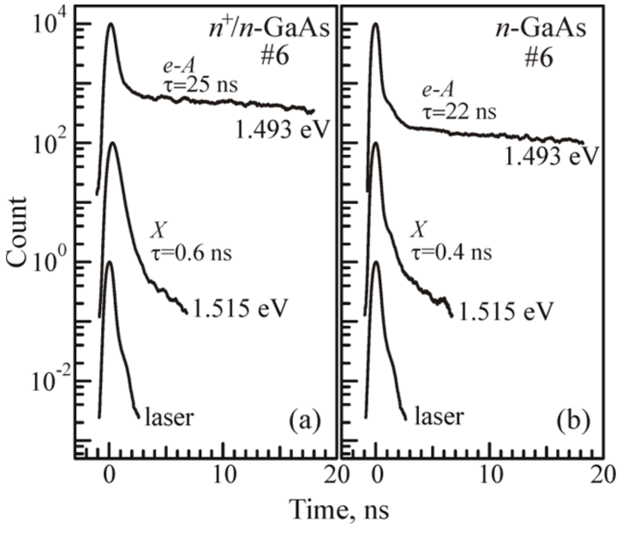

Fig. 2. The PL decay transients of different emission lines of (a) n^+/n-GaAs and (b) n-GaAs layers for sample #6 at T=3.6 K. The symbol X indicates free exciton transitions, and e-A denotes free electron-acceptor-related transitions. The lowest curve shows the laser excitation pulse. The decay time constants and line emission energies are marked at each trace. The curves are shifted vertically for clarity.

The initial part is very fast and is related to the free carrier capturing in excitons and defects. The second part is related to the free electron recombination via acceptor impurities. The characteristic emission time is equal to about $\tau_{e\text{-}A} = 22–25$ ns.

Figure 3 shows the temperature dependence of PL decay transients of excitonic emission lines *X* of (a) n^+/n-GaAs and (b) *n*-GaAs layers in sample #6. The excitonic emission in GaAs is considered up to a temperature of liquid nitrogen 77 K [16], and an increase in the excitonic lifetime from 0.4 to 0.6 ns for the *n*-GaAs layer and from 0.6 to 1.2 ns for the n^+/n-GaAs structure in the temperature range from 3.6 to 40 K, respectively, is observed (Fig. 3).

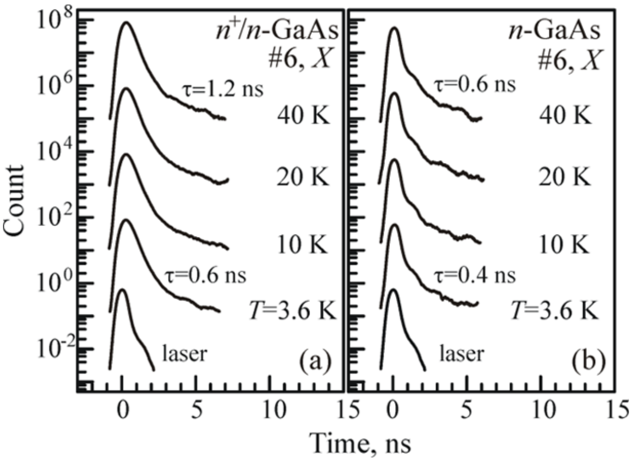

Fig. 3. The temperature dependence of the PL decay transients of excitonic emission lines *X* of (a) n^+/n-GaAs and (b) *n*-GaAs layers for sample #6. The lowest curve shows the laser excitation pulse. The curves are shifted vertically for clarity.

Figure 4 shows the PL time evolution of the different emission bands of (a) n^+/n-$Al_{0.3}Ga_{0.7}As$ and (b) *n*-$Al_{0.3}Ga_{0.7}As$ layers in sample #1 after pulsed laser excitation at a temperature of $T = 3.6$ K. The free excitonic emission decay time for both the *n*-$Al_{0.3}Ga_{0.7}As$ and the n^+/n-$Al_{0.3}Ga_{0.7}As$ structures is similar and equal to 0.5 ns. The evolution time of the free electron-acceptor emission characteristic varies from 4 to 15 ns, and it depends on the origin of the acceptor and on the structure itself. Some of the free carriers can drift to the energetically lower regions of the structure (e. g. GaAs) which can influence the free carrier concentration in the energetically higher region ($Al_{0.3}Ga_{0.7}As$).

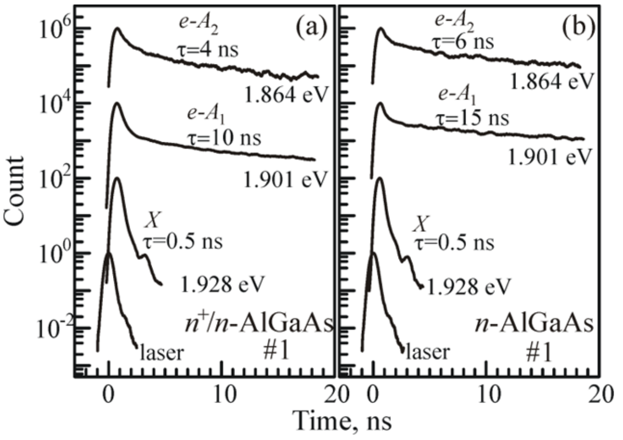

Fig. 4. The PL decay transients of different emission bands of (a) n^+/n-$Al_{0.3}Ga_{0.7}As$ and (b) *n*-$Al_{0.3}Ga_{0.7}As$ layers for sample #1 at $T = 3.6$ K. The symbol *X* indicates free exciton transitions, and *e*-A_1 and *e*-A_2 denote acceptor-related transitions. The lowest curve shows the laser excitation pulse. The decay time constants and emission energies are marked at each trace. The curves are shifted vertically for clarity.

Figure 5 shows a more detailed time scale of the PL time evolution of the excitonic *X* and electron-acceptor *e*-A_1 emission bands of the n^+/n-$Al_{0.3}Ga_{0.7}A$ structure (sample #1) at $T = 3.6$ K. At the energy of 1.78 eV, the broad emission band in a continuous wave PL spectrum of the $Al_{0.3}Ga_{0.7}As$ layer was

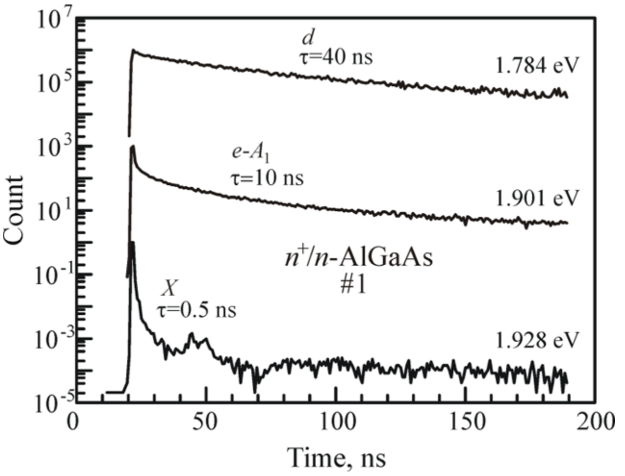

Fig. 5. The PL decay transients of different emission bands of n^+/n-$Al_{0.3}Ga_{0.7}A$ layers for sample #1 at $T = 3.6$ K. The symbol *d* indicates defect-related transitions, *e*-A_1 denotes acceptor-related transitions, and *X* indicates free exciton transitions. The decay time constants and emission energies are marked at each trace. The curves are shifted vertically for clarity.

observed (see Fig. 1). This broad band emission was attributed to point defects or complexes of Si with point defects [13]. The measurement of the emission lifetime of the defect-related emission *d*, which is also presented in Fig. 5, confirms that this emission is related to a deep defect level. The decay emission curve is not purely exponentional; however, the central part of the curve was approximated by an exponent. More details about estimation of local energetic levels can be found in Ref. [17]. The extracted characteristic emission lifetime is relatively long and equals about 40 ns. This lifetime was the longest one found in the structures that were investigated.

Figure 6 shows the temperature dependence of (a) excitonic X and (b) free electron-acceptor $e\text{-}A_1$ PL decay transients in the $n^+/n\text{-Al}_{0.3}\text{Ga}_{0.7}\text{As}$ structure of sample #1. The excitonic decay lifetime is nearly independent of temperature, and the free electron-acceptor decay lifetime is also found to be independent at temperatures up to 20 K. At higher temperatures $T \geq 40$ K, the free electron-acceptor decay time gets shorter since the thermal ionization of acceptors and other recombination channels (such as band–band recombination) starts dominating.

4. Discussion

The radiative lifetime of free excitons in ultrapure GaAs is 3.3 ns at the threshold of very low temperatures (1.7 K) [18]. The free exciton radiative characteristic time constant in our investigated structures is about 0.5 ns. This behaviour implies the existence of other radiative and nonradiative recombination channels.

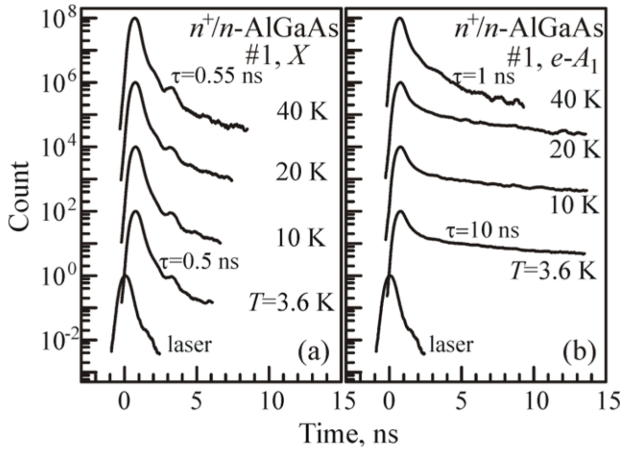

Fig. 6. The temperature dependence of (a) excitonic X and (b) free electron-acceptor $e\text{-}A_1$ PL decay transients in the $n^+/n\text{-Al}_{0.3}\text{Ga}_{0.7}\text{As}$ layer of sample #1. The lowest curve indicates the laser excitation pulse. The curves are shifted vertically for clarity.

In a previous publication [13], the enhancement of the continuous wave PL emission intensity in n^+/n-GaAs and $n^+/n\text{-Al}_{0.3}\text{Ga}_{0.7}\text{As}$ homojunction regions of these structures was reported. A comparison of the emission from n-GaAs and $n\text{-Al}_x\text{Ga}_{1-x}\text{As}$ layers with the emission from those being in contact with heavily doped layers revealed that the emission lines from the homojunctions were more intensive. The experiment showed that the contact of n-GaAs with n^+-GaAs and $n\text{-Al}_x\text{Ga}_{1-x}\text{As}$ with $n^+\text{-Al}_x\text{Ga}_{1-x}\text{As}$ gives rise to the intensity of PL spectra by about 10 and 20 times, respectively.

Similar effects were observed in Si-doped n^+/n-GaAs homojunction structures [19], Si δ-doped GaAs structures [20], in selectively Si-doped GaAs/AlGaAs heterostructures [21] as well as in AlInN/GaN heterostructures [22]. Theoretical calculations show that a strong electric field is induced in all of these structures at the interface side of the active layer. A good correlation was also shown between the calculated built-in electric field strength and the measured enhancement of the excitonic line intensity.

The incident laser beam generates electron–hole pairs at a certain depth of light penetration, and the photogenerated carriers can form excitons in the n-GaAs (or n-AlGaAs) layer. These in turn may recombine back by emitting photons. However, the presence of a strong built-in electric field prevents exciton formation in the close proximity to the n^+/n interface region where electric fields above 1 kV/cm destroy excitons by electron tunnelling. Consequently, holes are driven away from the interface, while the electrons drift towards the interface in the flat band region of the n-GaAs (or n-AlGaAs) layer. In the flat band region the accumulation of free carriers is initiated and the number of excitons is increased. The enhancement of free carrier concentration change the emission rate and quantum yield. This may explain in part the observed enhancement of the excitonic line intensity in the n^+/n-GaAs (or $n^+/n\text{-Al}_{0.3}\text{Ga}_{0.7}\text{As}$) homojunctions. The concentration change in free carriers leads to a redistribution between the emission channels because the excitonic emission intensity depends on the square law of the free carrier concentration. However, the impurity or defect-related recombination intensity has a linear dependence on the free carrier concentration [23].

Our experimental results shows that drift processes are important aspects to consider in the formation of excitons in n^+/n-GaAs and n^+/n-$Al_{0.3}Ga_{0.7}As$ flat band regions. Figure 7 shows a comparison of the excitonic *X* PL rise and decay transients in *n*-GaAs (dotted curve) and n^+/n-GaAs layers (solid curve) of sample #6 (*a*), as well as *n*-$Al_{0.3}Ga_{0.7}As$ (dotted curve) and n^+/n-$Al_{0.3}Ga_{0.7}As$ layers (solid curve) of sample #1 (*b*). The PL maximum of both n^+/n structures is shifted by about 200 ps. This fact indicates that an additional time (approximately a few hundred picoseconds) is required to accumulate free carriers in the flat band region of the homojunction structures. A similar result of free exciton dynamics was obtained in modulation-doped GaAs/AlGaAs structures [24]. There exists another explanation that relates the enhancement of the PL with the elimination of surface recombination [25]. However, this model cannot fully explain the excitonic emission enhancement observed at low temperatures. More widely this problem has also previously been discussed in literature [19].

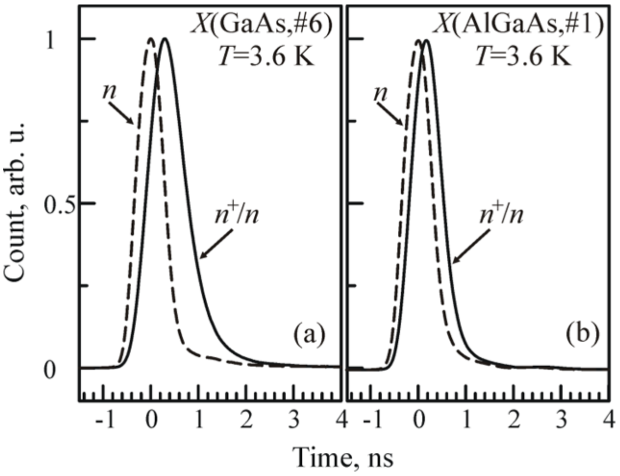

Fig. 7. Comparison of the excitonic *X* PL rise and decay transients in (a) *n*-GaAs (dotted curve) and n^+/n-GaAs (solid curve) for sample #6 and in (b) *n*-$Al_{0.3}Ga_{0.7}As$ (dotted curve) and n^+/n-$Al_{0.3}Ga_{0.7}As$ (solid curve) for sample #1.

5. Conclusions

The PL spectra and light emission lifetimes in GaAs/$Al_{0.3}Ga_{0.7}As$ structures designed for MW and THz detectors were investigated, and possible mechanisms of carrier recombination have been discussed. The measured free exciton emission characteristic time was found to be 0.5 ns at a temperature of 3.6 K. The free electron-acceptor recombination lifetime was 22–25 ns in the GaAs structures and 4–15 ns in the AlGaAs structures. The emission lifetime of deep Si level having a 170 meV activation energy in the AlGaAs layer was found to be equal to 40 ns. The excitonic PL maximum of n^+/n-GaAs and n^+/n-$Al_{0.3}Ga_{0.7}As$ homojunction structures offers delays of approximately 200 ps compared to *n*-GaAs and *n*-$Al_{0.3}Ga_{0.7}As$ structures. This indicates that the free carrier drift is an important factor in the formation of free excitons in the *n*-GaAs and *n*-$Al_{0.3}Ga_{0.7}As$ layers of the homojunction structures.

Acknowledgements

This work was in part supported by the Agency for Science, Innovation and Technology (grant No. 31V-32) in the frame of the High Technology Development Programme for 2011–2013. The authors kindly acknowledge Gytis Steikūnas and Angelė Steikūnienė for the preparation of the samples.

References

[1] P.H. Siegel, Terahertz technology in biology and medicine, IEEE Trans. Microw. Theory Tech. **52**(10), 2438–2447 (2004).

[2] J. Federici and L. Moeller, Review of terahertz and subterahertz wireless communications, J. Appl. Phys. **107**(11), 111101–22 (2010).

[3] H. Takeuchi, J. Yanagisawa, T. Hasegawa, and M. Nakayama, Enhancement of terahertz electromagnetic wave emission from an undoped GaAs/*n*-type GaAs epitaxial layer structure, Appl. Phys. Lett. **93**(8), 081916–3 (2008).

[4] A. Reklaitis, Comparison of efficiencies of GaAs-based pulsed terahertz emitters, J. Appl. Phys. **101**(11), 116104–3 (2007).

[5] A.G.U. Perera, H.X. Yuan, S.K. Gamage, W.Z. Shen, M.H. Francombe, H.C. Liu, M. Buchanan, and W.J. Schaff, GaAs multilayer p^+-*i* homojunction far-infrared detectors, J. Appl. Phys. **81**(7), 3316–3319 (1997).

[6] A.G.U. Perera, in: *Semiconductors and Semimetals*, Vol. 84, eds. S.D. Gunapala, D.R. Rhiger, and C. Jagadish (Academic Press, San Diego, 2011) pp. 243–302.

[7] A.B. Weerasekara, M.B.M. Rinzan, R.C. Jayasinghe, S.G. Matsik, A.G.U. Perera, M. Buchanan, H.C. Liu, G. von Winckel, A. Stintz, and S. Krishna, Single and multi emitter terahertz detectors using n-type GaAs/AlGaAs heterostructures, IEEE Sensors 2007 Conference, 507–510 (2007).

[8] A. Sužiedėlis, S. Ašmontas, J. Kundrotas, J. Gradauskas, E. Širmulis, A. Čerškus, and V. Nargelienė, Planar heterojunction diodes for microwave and infrared applications, in: *Advanced Optical Materials and Devices (AOMD-7): 7th International Conference: Vilnius, Lithuania, 28–31 August, 2011: Program and Abstracts* (Vilnius, 2011) p. 74.

[9] A.Y. Cho, Growth and properties of III–V semiconductors by molecular beam epitaxy, in: *Molecular Beam Epitaxy and Heterostructures*, eds. L.L. Chang and K. Ploog (Martinus Nijhoff Publishers, Dordrecht, 1985) pp. 191–226.

[10] W.T. Tsang, Molecular beam epitaxy for III–V compound semiconductors, in: *Semiconductors and Semimetals*, Vol. 22, Part A, ed. W.T. Tsang (Academic Press, London, 1985) pp. 95-207.

[11] W. Becker, *Advanced Time-Correlated Single Photon Counting Techniques* (Springer Berlin Heidelberg, New York, 2005).

[12] S.B. Nam, D.C. Reynolds, C.W. Litton, R.J. Almassy, T.C. Collins, and C.M. Wolfe, Free-exciton energy spectrum in GaAs, Phys. Rev. B **13**(2), 761–767 (1976).

[13] A. Čerškus, J. Kundrotas, V. Nargelienė, A. Sužiedėlis, S. Ašmontas, J. Gradauskas, A. Johannessen, and E. Johannessen, Photoluminescence characterisation of GaAs/AlGaAs structures designed for microwave and terahertz detectors, Lith. J. Phys. **51**(4), 330–334 (2011).

[14] D. V. O'Connor and D. Phillips, *Time-Correlated Single Photon Counting* (Academic Press, London, 1984).

[15] Origin: Convolution/Deconvolution Example. URL: http://www.originlab.com/index.aspx?go=Products/Origin/DataAnalysis/SignalProcessing/Convolution&pid=67.

[16] E. Grilli, M. Guzzi, R. Zamboni, and L. Pavesi, High-precision determination of the temperature dependence of the fundamental energy gap in gallium arsenide, Phys. Rev. B **45**(4), 1638–1644 (1992).

[17] J. Vaitkus and J. Viščakas, On the determination of parameters of defect levels, Lith. J. Phys. **6**(1), 65 (1966).

[18] G.W. 't Hooft, W.A.J.A. van der Poel, L.W. Molenkamp, and C.T. Foxon, Giant oscillator strength of free excitons in GaAs, Phys. Rev. B **35**(15), 8281–8284 (1987).

[19] A. Čerškus, V. Nargelienė, J. Kundrotas, A. Sužiedėlis, S. Ašmontas, J. Gradauskas, A. Johannessen, and E. Johannessen, Enhancement of the excitonic photoluminescence in n^+/i-GaAs by controlling the thickness and impurity concentration of the n^+ layer, Acta Phys. Pol. A **119**(2), 154–157 (2011).

[20] V. Nargelienė, S. Ašmontas, A. Čerškus, J. Gradauskas, J. Kundrotas, and A. Sužiedėlis, Peculiarities of excitonic photoluminescence in Si δ-doped GaAs structures, Acta Phys. Pol. A **119**(2), 177–179 (2011).

[21] J. Kundrotas, A. Čerškus, V. Nargelienė, A. Sužiedėlis, S. Ašmontas, J. Gradauskas, A. Johannessen, E. Johannessen, and V. Umansky, Enhanced exciton photoluminescence in the selectively Si-doped GaAs/Al$_x$Ga$_{1-x}$As heterostructures, J. Appl. Phys. **108**(6), 063522–7 (2010).

[22] J. Kundrotas, A. Čerškus, J. Liberis, A. Matulionis, J.H. Leach, and A.H. Morkoç, Enhancement and narrowing of excitonic lines in AlInN/GaN heterostructures, Acta Phys. Pol. A **119**(2), 173–176 (2011).

[23] T. Schmidt, K. Lischka, and W. Zulehner, Excitation-power dependence of the near-band edge photoluminescence of semiconductors, Phys. Rev. B **45**(16), 8989–8994 (1992).

[24] J.X. Shen, R. Pittini, Y. Oka, and E. Kurtz, Exciton dynamics in GaAs/Ga$_{1-x}$Al$_x$As heterojunctions and GaAs epilayers, Phys Rev. B **61**(4), 2765–2772 (2000).

[25] L.M. Smith, D.J. Wolford, R. Venkatasubramanian, and S.K. Ghandhi, Radiative recombination in surface-free $n^+/n^-/n^+$ GaAs homostructures, Appl. Phys. Lett. **57**(15), 1572–1574 (1990).

MIKROBANGŲ IR TERAHERCŲ DETEKTORIAMS SKIRTŲ GaAs/$Al_{0,3}Ga_{0,7}As$ DARINIŲ FOTOLIUMINESCENCIJOS TRUKMĖS

A. Čerškus [a, b], J. Kundrotas [a], V. Nargelienė [a], A. Sužiedėlis [a], S. Ašmontas [a], J. Gradauskas [a],
E. Johannessen [c], A. Johannessen [c]

[a] *Fizinių ir technologijos mokslų centro Puslaidininkių fizikos institutas, Vilnius, Lietuva*

[b] *Lietuvos edukologijos universitetas, Vilnius, Lietuva*

[c] *Vestfoldo universitetinis koledžas, Borre, Norvegija*

Santrauka

Ištirta Si donorais legiruotų GaAs/$Al_{0,3}Ga_{0,7}As$ darinių, skirtų mikrobangų ir terahercų detektoriams, fotoliuminescencija ir šviesos emisijos trukmė esant stipriai legiruotiems sluoksniams bei šiuos sluoksnius nuėsdinus. Tyrimams naudotos dvi metodikos: nuostoviosios fotoliuminescencijos ir pavienių koreliuotų fotonų skaičiavimo metodika. Tyrimai atlikti temperatūrose tarp 3,6 ir 77 K. $Al_{0,3}Ga_{0,7}As$ spektre nustatytos dviejų tipų priemaišinės linijos, susijusios su sekliosiomis anglies C ir silicio Si akceptorinėmis priemaišomis. Ištirta GaAs ir $Al_{0,3}Ga_{0,7}As$ eksitoninių ir priemaišinių linijų emisijos trukmė. Nustatyta, kad eksitoninės emisijos trukmė lygi 0,5 ns esant 3,6 K temperatūrai. Laisvųjų elektronų rekombinacijos su akceptoriais emisijos trukmė GaAs sluoksniuose siekė 22–25 ns, o $Al_{0,3}Ga_{0,7}As$ sluoksniuose buvo 4–15 ns. Ištirtas gilus emisijos centras $Al_{0,3}Ga_{0,7}As$ sluoksnyje: jo aktyvacijos energija lygi 170 meV, o emisijos trukmė – 40 ns. Šis centras susietas su taškinių defektų arba kompleksų tarp Si ir taškinių defektų susidarymu n^+-$Al_{0,3}Ga_{0,7}As$ sluoksniuose. Aptiktas GaAs ir $Al_{0,3}Ga_{0,7}As$ spektrinių linijų intensyvumo sustiprėjimas. Šis sustiprėjimas siejamas su n^+/n sandūrų įtaka šiuose dariniuose; tai patvirtina ir emisijos vėlinimas apie 200 ps esant n^+/n sandūroms, palyginti su emisija GaAs ar $Al_{0,3}Ga_{0,7}As$ sluoksniuose. Taigi eksitonų formavimui n^+/n dariniuose yra svarbus laisvųjų krūvininkų dreifas į silpnojo lauko sritį, kurioje jie padidina eksitonų tankį ir taip sustiprina eksitoninę spinduliuotę.